Electrical characterization of defects introduced in *n*-type N-doped 4H-SiC during electron beam exposure

Ezekiel Omotoso[1, 2, a *], Walter Ernst Meyer[1, b], Francois Danie Auret[1, c],
Sergio Manuel Martins Coelho[1, d], and Phuti Ngako Mahloka Ngoepe[1, f]
[1] Department of Physics, University of Pretoria, Private Bag X20, Hatfield 0028, South Africa
[2] Departments of Physics, Obafemi Awolowo University, Ile-Ife, 220005, Nigeria
[a]ezekiel.omotoso@up.ac.za, [b]wmeyer@up.ac.za, [c]danie.auret@up.ac.za,
[d]Sergio.coelho@up.ac.za, [f]phuti.ngoepe@up.ac.za

Keywords: silicon carbide, defects, deep level transient spectroscopy, electron beam exposure

Abstract. Deep level transient spectroscopy (DLTS) was used to characterize the defects introduced in *n*-type, N-doped, 4H-SiC while being exposed to electron beam evaporation conditions. This was done by heating a tungsten source using an electron beam current of 100 mA, which was not sufficient to evaporate tungsten. Two new defects were introduced during the exposure of 4H-SiC samples to electron beam deposition conditions (without metal deposition) after resistively evaporated nickel Schottky contacts. We established the identity of these defects by comparing their *signatures* to those of high energy particle irradiation induced defects of the same materials. The defect $E_{0.42}$ had acceptor-like behaviour and could be attributed to be a silicon or carbon vacancy. The $E_{0.71}$ had intrinsic nature and was linked to a carbon vacancy and/or carbon interstials.

Introduction

Metallization is a very important processing step in the microelectronics and photovoltaic industries. Electron beam deposition is one of the popular techniques in the fabrication of ohmic and Schottky barrier contacts at high controllable rate. Auret *et al* [1] and Coelho *et al* [2] have reported that metallization procedures, including electron beam deposition (EBD), induced defects at and close to the metal-semiconductor junction [3]. These defects influence the performance of the devices and alter the contacts' Schottky barrier heights [4].

The defects introduced by the electron beam when energetic particles interact with the semiconductor surface will lead to lattice damage depending on the energy and duration of the exposure. These defects may either be of benefit or detrimental to device performance.

Silicon carbide (SiC) has drawn the interest of many researchers due to its wide bandgap of 3.4 eV [5] and the excellent properties such as high thermal conductivity, high breakdown field and high saturated drift velocity [6]. These characteristics make SiC a very good semiconductor capable of outperforming silicon in electronic devices for high-power, high-frequency and high-temperature applications [7]. SiC is also a key material for next-generation photonics [8].

In this paper, we have investigated the effect of exposing nitrogen-doped, n-type 4H-SiC to electron beam conditions (without metal deposition) prior to metal deposition by resistive evaporation. The motivation is mainly to study the influence of electron beam exposure (EBE) on the 4H-SiC semiconductor and the signatures of the defects present after the deposition of nickel Schottky contacts. The defects emanated were compared with the defects in as-grown SiC and SiC after bombardment with alpha-particles from a ^{241}Am source and by high energy electrons from a ^{90}Sr source.

Experimental Procedure

We have used an *n*-type, N-doped 4H-SiC wafer, double polished with Si face epi-layer, resistivity of 0.02 Ω-cm and doping density of 7.1×10^{15} cm^{-2}. The 4H-SiC wafer was supplied by CREE Res. Inc. Prior to metallization, the samples were cut into smaller pieces with dimensions of approximately 4 mm × 2 mm. The samples were degreased by boiling for 5 minutes each in trichloroethylene, acetone, methanol and followed by 1 minute rinse in de-ionized water. They were also etched in a 40% concentration of HF for 30 seconds in order to remove the native oxide layer on the samples, and then rinsed in de-ionized water, followed by blowing dry with nitrogen gas as reported earlier by Omotoso *et al* [9].

Directly after cleaning, the samples were mounted on a metal contact mask and inserted into the vacuum chamber that was pumped down to 10^{-5} mbar before thermal evaporation of Ni ohmic contacts onto the highly doped (1.0×10^{18} cm^{-3}) back surface of the samples. Ohmic contact was evaporated at a deposition rate of 0.9 Å s^{-1} for approximately 30 minutes to achieve the thickness of 3000 Å. The samples were annealed in a tube furnace under flowing argon gas at 950℃ for 10 minutes to form nickel silicides [10] in order to reduce the contact resistance, thus forming an ohmic contact.

The cleaning procedures were repeated after annealing of the ohmic contact but only for three minutes in an ultrasonic bath. The samples were also dried with nitrogen gas before the fabrication of nickel Schottky barrier diodes (SBDs). SBDs were fabricated in two stages: nickel Schottky contacts, 0.6 mm in diameter and of thickness 100 Å were first deposited by resistive evaporation technique before being quickly transferred into the electron beam deposition chamber for exposure to the electron beam. Electron beam exposure (EBE) of the samples was achieved by using a 10 kV source (MDC model e-Vap 10CVS) with samples placed 50 cm away from the metal crucible as earlier reported by Auret et al [1] and Coelho et al [2]. The samples were exposed to EBE conditions for 50 minutes from a heated tungsten source using a beam current of 100 mA and an acceleration voltage of 10 kV [2]. This current was not enough to evaporate tungsten, but would have been sufficient to evaporate most other metals. During the entire exposure, the vacuum in the deposition chamber was reduced to 10^{-4} mbar by leaking in forming gas H15 (N_2:H_2 of 85%:15% by volume) [2].

Hereafter, the samples were removed and returned quickly to the resistive deposition chamber. Additional Ni was deposited resulting in thickness of 1000 Å Schottky diodes and an area of 2.8×10^{-3} cm^2 were deposited at a rate of 0.2 Å s^{-1} and a vacuum of approximately 5×10^{-6} mbar by means of resistive evaporation, a process known to not introduce defects measurable by DLTS [2].

Subsequent to SBD fabrication, current-voltage (*I*-*V*) and capacitance-voltage (*C*-*V*) measurements were carried out to determine the quality of the diodes. The *I*-*V* and *C*-*V* measurements were carried out by an HP 4140 B pA meter/DC voltage source and an HP 4192A LF Impedance Analyzer, respectively. The defects introduced into the samples were thereafter characterised by conventional deep level transient spectroscopy (DLTS). The DLTS spectra were recorded over the temperature range 30 – 350 K, at a quiescent reverse bias of –5.0 V, filling pulse height of amplitude 6 V, filling pulse width of 2.0 ms and at different rate windows, in order to determine the defect signatures by means of Arrhenius plots.

In order to aid identification of the defects introduced by EBE, they were compared to the defects present in resistively deposited SBDs as-grown, irradiated by alpha-particles (with energy of approximately 5.4 MeV) from an ^{241}Am radio-nuclide and high energy electrons (above 200 keV). The alpha particle irradiation was done at a fluence rate of 7×10^{6} cm^{-2} s^{-1} for 2 hours to obtain a fluence of 5×10^{10} alpha-particles-cm^{-2}. The ^{90}Sr radionuclides used decay first to Y with the emission of an 0.5 MeVelectron of halflife of 28.5 years and then decay to Zr with the emission of a 2.3 MeV electron of halflife of 64.1 hours [11]. The ^{90}Sr radio-nuclide source had a fluence rate of 1×10^{9} electrons-cm^{-2} s^{-1} with energies above 200 keV. Here the sample was irradiated for 24 hours in order to obtain a fluence of 2×10^{10} electron-cm^{-2}.

Results and Discussion

Defects in as-grown 4H-SiC

The defects introduced during the EBE were compared with defects present in as-grown SiC, as well as defects introduced by alpha-particle and high energy electron irradiation. It has been reported in literature that RE does not introduced defect in measurable quantities [2]. Therefore, this technique was employed to evaporate nickel on n-type 4H-SiC for both ohmic and Schottky contacts because of aforementioned advantage. The electrical characteristics of the Schottky contacts are summarised in Table 1. The DLTS spectrum of the control sample recorded at a rate window of 20 s^{-1} is shown in Fig. 1. The spectrum showed the presence of four defect levels, labelled $E_{0.10}$, $E_{0.12}$, $E_{0.16}$ and $E_{0.65}$, where "E" refers to an electron trap and the number at the subscript say 0.10, is the activation enthalpy of the defect below the conduction band. Both the activation enthalpy and the corresponding apparent capture cross section, referred to as the defect's *signature*, were determined from the Arrhenius plots, and are tabulated in Table 2.

Table 1 Comparison of electrical characteristics of Ni/4H-SiC Schottky barrier diodes for different processes.

Samples	n	I_s [A]	R_s [Ω]	V_{bi} [V]	N_D [cm^{-3}]	$\phi_{I\text{-}V}$ [eV]	$\phi_{C\text{-}V}$ [eV]
As-grown	1.04	15.5×10^{-18}	48	1.07	7.8×10^{15}	1.25	1.36
α-particle irradiation	1.07	2.6×10^{-18}	270	1.23	7.4×10^{15}	1.31	1.52
HEE irradiation	1.13	1.4×10^{-19}	60	1.32	6.8×10^{15}	1.38	1.60
EBE	1.26	6.6×10^{-17}	13	1.41	8.0×10^{15}	1.21	1.68

Table 2 Electronic properties of defects detected by DLTS in Ni/4H-SiC SBD after various processing steps.

Process	Defect label	E_T [eV]	σ_a [cm^2]	T_{20} [K]	Defect ID	Refs.
RE	$E_{0.10}$	$E_C - 0.10$	3×10^{-12}	45	N	[12]
	$E_{0.12}$	$E_C - 0.12$	1×10^{-15}	65	Ti	[13]
	$E_{0.16}$	$E_C - 0.16$	1×10^{-15}	85	Ti	[14]
	$E_{0.65}$	$E_C - 0.65$	4×10^{-15}	304	$V_{C/Si}$ (Z_1/Z_2)	[14, 15]
α-particle	$E_{0.10}$	$E_C - 0.10$	2×10^{-12}	44	N	[12]
	$E_{0.12}$	$E_C - 0.12$	1×10^{-15}	65	Ti	[13]
	$E_{0.16}$	$E_C - 0.16$	3×10^{-15}	85	Ti	[14]
	$E_{0.39}$	$E_C - 0.39$	2×10^{-15}	192	$V_{C/Si}$	[16]
	$E_{0.61}$	$E_C - 0.61$	5×10^{-15}	302	$V_{C/Si}$ (Z_1/Z_2)	[12, 17]
	$E_{0.70}$	$E_C - 0.70$	6×10^{-15}	333	$V_{C/Si}$ (Z_1/Z_2)	[14, 15]
HEE	$E_{0.10}$	$E_C - 0.10$	1×10^{-16}	44	N	[12]
	$E_{0.12}$	$E_C - 0.12$	4×10^{-12}	65	Ti	[13]
	$E_{0.16}$	$E_C - 0.16$	1×10^{-15}	84	Ti	[14]
	$E_{0.22}$	$E_C - 0.22$	2×10^{-17}	141	?	?
	$E_{0.40}$	$E_C - 0.40$	3×10^{-15}	199	$V_{C/Si}$	[16]
	$E_{0.65}$	$E_C - 0.65$	3×10^{-15}	300	$V_{C/Si}$ (Z_1/Z_2)	[14, 15]
	$E_{0.70}$	$E_C - 0.70$	3×10^{-15}	338	$V_{C/Si}$ (Z_1/Z_2)	[14, 15]
EBE	$E_{0.10}$	$E_C - 0.10$	1×10^{-11}	44	N	[12]
	$E_{0.12}$	$E_C - 0.12$	2×10^{-16}	64	Ti	[13]
	$E_{0.16}$	$E_C - 0.16$	2×10^{-15}	84	Ti	[14]
	$E_{0.42}$	$E_C - 0.42$	5×10^{-15}	201	$V_{C/Si}$	[16]
	$E_{0.66}$	$E_C - 0.66$	4×10^{-15}	302	$V_{C/Si}$ (Z_1/Z_2)	[14, 15]
	$E_{0.71}$	$E_C - 0.71$	1×10^{-15}	340	$V_{C/Si}$ (Z_1/Z_2)	[14, 15]

Alpha-particle irradiation

The electrical characteristics of the diode after irradiation are shown in Table 1. The diode was still of good quality after irradiation. The deep levels introduced by irradiation were also characterised by DLTS (see Fig. 1). Alpha-particle irradiated SBD introduced two defects ($E_{0.39}$ and $E_{0.62}$) with complicated broad peaks. The activation energies of the two defects are 0.39 and 0.62 eV, respectively. The attributes of the defects were tabulated in Table 2.

High energy electron (HEE) irradiation

The results obtained from the *I-V* and *C-V* measurements as shown in Table 1 confirmed the suitability of the SBDs for DLTS measurements. As already reported, high energy electron irradiation of 4H-SiC yields three new defects [9]. The peaks could be attributed to vacancies in both silicon and carbon sublattices deepening on the energy required to displace the relevant atom [18]. The broadness of the peaks may be as a result of superposition of several peaks that have closely spaced activation energies. Point defects are formed due to the low mass of the electron relative to the nucleus since the recoiling nucleus does not have enough kinetic energy to cause further displacements [11]. The attribute of the defects introduced by high energy electrons are also tabulated in Table 2.

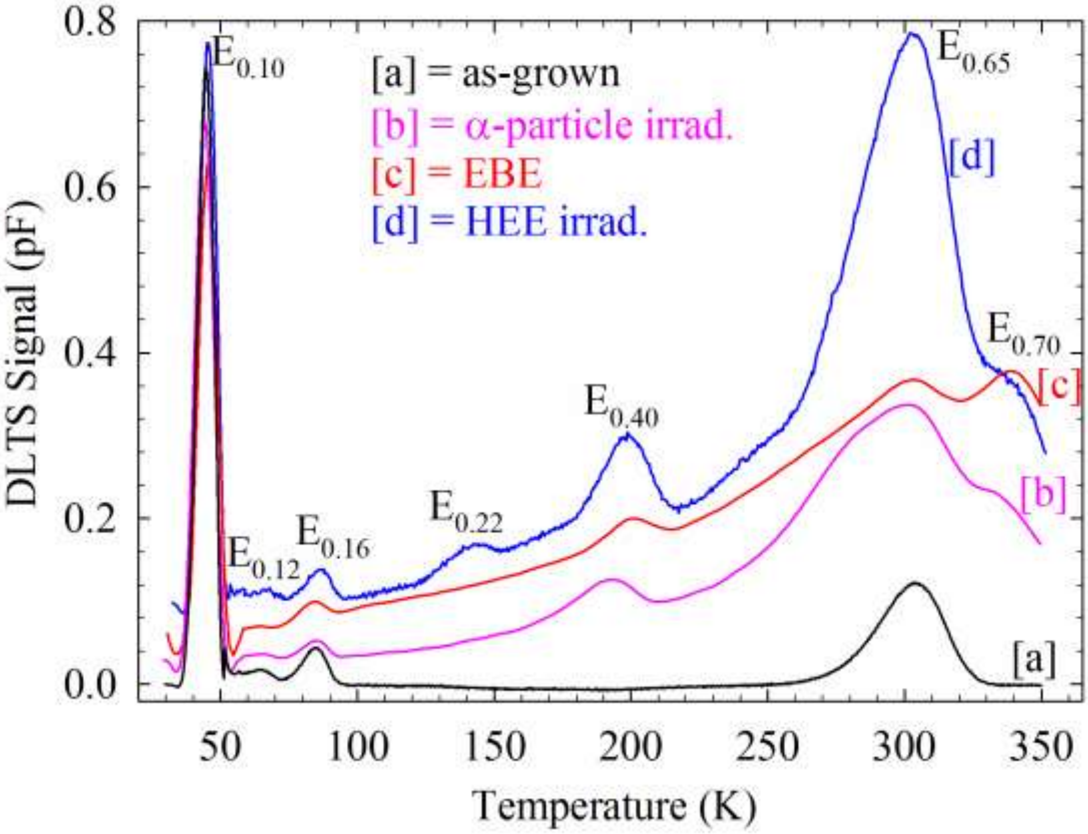

Fig. 1: DLTS spectra of Ni/4H-SiC for: [a] as-grown; [b] irradiated with α-particles; [c] exposed to electron beam condition without metal deposition (EBE); [d] irradiated with high energy electrons.

Electron beam exposure, without metal deposition

In most experimental setups in electron beam evaporators, the position of the sample and the sample holder during the pre-metallization heating and degassing of the metal may be varied. The sample may be rotated to face away from the crucible or shield the sample with a shutter during the experimental procedure. This procedure may not be applicable to larger commercial systems where metallization of large areas is required. In this section, we investigate the effect of exposing a 4H-SiC sample to electron beam deposition conditions, however, *without metal deposition*.

The electrical characteristics of the EBE exposed diode after deposition are shown in Table 1. It was noted that the carrier density as determined by *C-V* measurements was 8.0×10^{15} cm^{-3}.

In Fig. 2, we compare the spectra recorded using SBDs prepared by resistive evaporation of Ni (a), alpha-particle irradiated (b), high energy electron irradiated (c), and electron beam deposition conditions, *without metal deposition* (d). From the spectra, it was observed that the electron beam exposure introduced two defects which were similar to defects introduced by high energy particle irradiation but in lower concentration. We therefore conclude that exposure of samples to electron beam *without metal deposition* could be another mechanism of introducing defects $E_{0.42}$ and $E_{0.71}$ without bombardment with high energy particle irradiation. The defect $E_{0.42}$ was reported earlier by Doyle *et al* [16], who reported that it has acceptor-like behaviour. A similar defect level has been attributed to the silicon vacancy [19], carbon vacancy, split interstitial or antisites after low energy electron irradiation [18]. The $E_{0.71}$ is commonly known as the Z_1Z_2 defect. Defect $E_{0.71}$ has intrinsic nature and is linked to a carbon vacancy, carbon interstials and complexes of carbon vacancies and interstials [16, 20, 21]

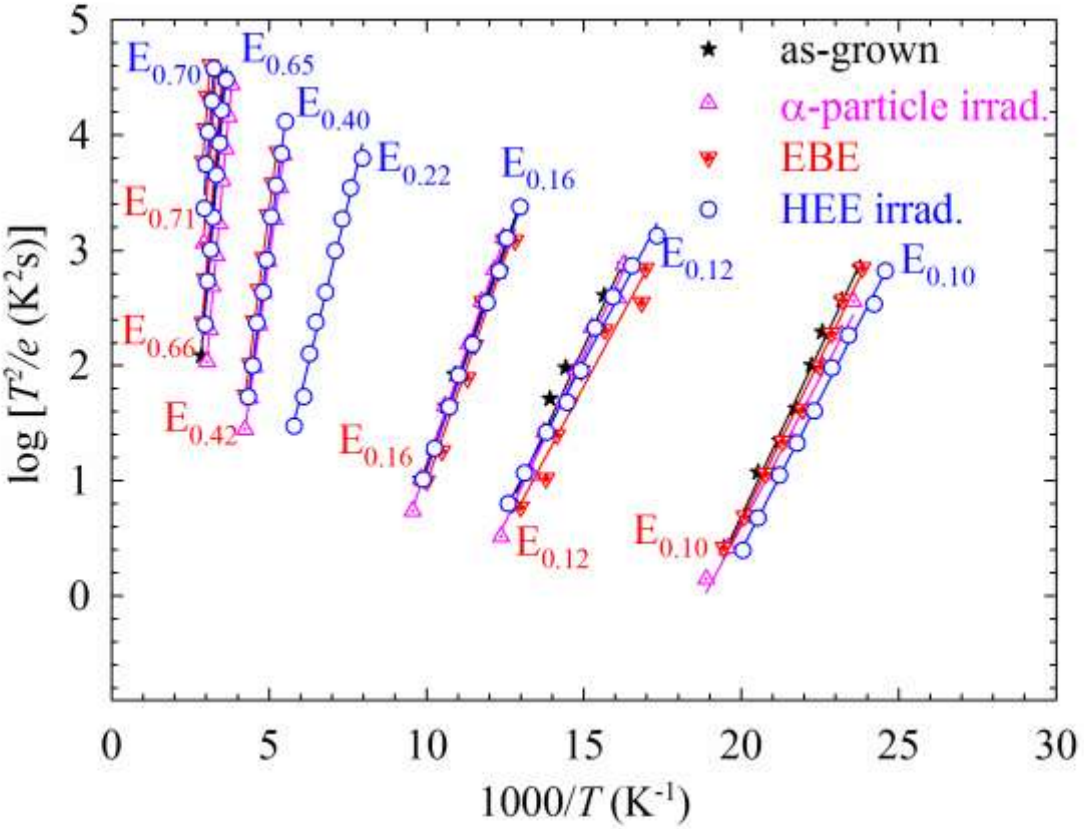

Fig. 2: Arrhenius plots of Ni/4H-SiC for: [a] as-grown ; [b] irradiated with α-particles; [c] exposed to electron beam condition without metal deposition (EBE); [d] irradiated with high energy electrons.

Conclusions

The current-voltage and the capacitance-voltage characteristics demonstrated that the Ni/4H-SiC SBDs prepared were suitable for the research. Deep level transient spectroscopy revealed the presence of four defects below the conduction band ($E_{0.10}$, $E_{0.12}$, $E_{0.16}$ and $E_{0.65}$) after resistive evaporation, which we conclude were in the as-grown material. We observed two additional defects, $E_{0.42}$ and $E_{0.71}$ after electron beam exposure, without metal deposition. The apparent capture cross sections of defects $E_{0.42}$ and $E_{0.71}$ were estimated from the intercept of the Arrhenius plot to be 5×10^{-15} cm^2 and 1×10^{-15} cm^2, respectively. The signatures of defects $E_{0.42}$ and $E_{0.71}$ are similar to defects induced as a result of high energy particles such as alpha-particle and high energy electron irradiation. The defect $E_{0.42}$ has acceptor-like behaviour and has also been attributed to the silicon or carbon vacancy. The defect $E_{0.71}$, known as Z_1Z_2, has intrinsic nature that is linked to a carbon vacancy, carbon interstials and complexes of carbon vacancies and interstials.

We therefore show that, although 10 keV electrons are not supposed to cause damage in SiC, EBE does cause damage near the sample surface, similar to that produced by high energy particles. It is therefore concluded that electron beam exposure is detrimental to device properties. Proper shielding as well as deposition of metal in the best possible vacuum should also be employed.

Acknowledgement

This work is based on the research supported in part by the National Research Foundation (NRF) of South African (Grant specific unique reference number (UID) 78838). The Grant holder acknowledges that opinions, findings and conclusions or recommendations expressed in this publication generated by the NRF supported are that of authors and that NRF accepts no liability whatsoever in this regard.

References

[1] F.D. Auret, S.M.M. Coelho, J.M. Nel, W.E. Meyer, Electrical characterization of defects introduced in n-Si during electron beam deposition of Pt, physica status solidi (a), 209 (2012) 1926-1933.
[2] S.M.M. Coelho, F.D. Auret, P.J. Janse van Rensburg, J.M. Nel, Electrical characterization of defects introduced in n-Ge during electron beam deposition or exposure, Journal of Applied Physics, 114 (2013) 1737081-1737088.
[3] F.D. Auret, P.M. Mooney, Deep levels introduced during electron-beam deposition of metals on n-type silicon, Journal of Applied Physics, 55 (1984) 988-993.
[4] G. Myburg, F. Auret, Influence of the electron beam evaporation rate of Pt and the semiconductor carrier density on the characteristics of Pt/n-GaAs Schottky contacts, Journal of applied physics, 71 (1992) 6172-6176.
[5] L.M. Tolbert, B. Ozpineci, S.K. Islam, M.S. Chinthavali, Wide bandgap semiconductors for utility applications, Power and Energy Systems, Proceedings, 1 (2003) 317-321.
[6] M. Siad, M. Abdesslam, A.C. Chami, Role of carbon in the formation of ohmic contact in Ni/4HSiC and Ni/Ti/4HSiC, Applied Surface Science, 258 (2012) 6819-6822.
[7] R. Madar, Materials science: Silicon carbide in contention, Nature, 430 (2004) 974-975.
[8] S. Yamada, B.-S. Song, T. Asano, S. Noda, Silicon carbide-based photonic crystal nanocavities for ultra-broadband operation from infrared to visible wavelengths, Applied Physics Letters, 99 (2011) 2011021-2011023.
[9] E. Omotoso, W.E. Meyer, F.D. Auret, A.T. Paradzah, M. Diale, S.M.M. Coelho, P.J. Janse van Rensburg, The influence of high energy electron irradiation on the Schottky barrier height and the Richardson constant of Ni/4H-SiC Schottky diodes, Materials Science in Semiconductor Processing, 39 (2015) 112-118.
[10] T. Marinova, A. Kakanakova-Georgieva, V. Krastev, R. Kakanakov, M. Neshev, L. Kassamakova, O. Noblanc, C. Arnodo, S. Cassette, C. Brylinski, B. Pecz, G. Radnoczi, G. Vincze, Nickel based ohmic contacts on SiC, Materials Science and Engineering: B, 46 (1997) 223-226.

[11] F. Auret, S. Goodman, G. Myburg, W. Meyer, Electrical characterization of defects introduced in n-GaAs by alpha and beta irradiation from radionuclides, Appl. Phys. A, 56 (1993) 547-553.
[12] T. Kimoto, A. Itoh, H. Matsunami, S. Sridhara, L. Clemen, R. Devaty, W. Choyke, T. Dalibor, C. Peppermüller, G. Pensl, Nitrogen donors and deep levels in high-quality 4H–SiC epilayers grown by chemical vapor deposition, Applied physics letters, 67 (1995) 2833-2835.
[13] A.A. Lebedev, Deep level centers in silicon carbide: A review, Semiconductors, 33 (1999) 107-130.
[14] T. Dalibor, G. Pensl, H. Matsunami, T. Kimoto, W.J. Choyke, A. Schöner, N. Nordell, Deep Defect Centers in Silicon Carbide Monitored with Deep Level Transient Spectroscopy, physica status solidi (a), 162 (1997) 199-225.
[15] I. Pintilie, L. Pintilie, K. Irmscher, B. Thomas, Formation of the Z1,2 deep-level defects in 4H-SiC epitaxial layers: Evidence for nitrogen participation, Applied Physics Letters, 81 (2002) 4841-4843.
[16] J. Doyle, M.K. Linnarsson, P. Pellegrino, N. Keskitalo, B. Svensson, A. Schoner, N. Nordell, J. Lindstrom, Electrically active point defects in n-type 4H–SiC, Journal of applied physics, 84 (1998) 1354-1357.
[17] G. Pensl, W.J. Choyke, Electrical and optical characterization of SiC, Physica B: Condensed Matter, 185 (1993) 264-283.
[18] L. Storasta, J.P. Bergman, E. Janzén, A. Henry, J. Lu, Deep levels created by low energy electron irradiation in 4H-SiC, Journal of Applied Physics, 96 (2004) 4909-4915.
[19] F. Nava, G. Bertuccio, A. Cavallini, E. Vittone, Silicon carbide and its use as a radiation detector material, Measurement Science and Technology, 19 (2008) 102001.
[20] C. Hemmingsson, N.T. Son, O. Kordina, J.P. Bergman, E. Janzén, J.L. Lindström, S. Savage, N. Nordell, Deep level defects in electron-irradiated 4H SiC epitaxial layers, Journal of Applied Physics, 81 (1997) 6155-6159.
[21] T.A.G. Eberlein, R. Jones, P.R. Briddon, Z_1/Z_2 Defects in 4H−SiC, Physical Review Letters, 90 (2003) 2255021-2255024.